Clinical Radiology 75 (2020) 876.e17–876.e32

Contents lists available at ScienceDirect

Clinical Radiology

journal homepage: www.clinicalradiologyonline.net

Pictorial Review

Intramedullary tumours and tumour mimics

S.G. Kandemirli [a,*], A. Reddy [a], P. Hitchon [b], J. Saini [c], G. Bathla [a]

[a] University of Iowa Hospital and Clinics, Department of Radiology, Iowa city, IOWA, USA
[b] University of Iowa Hospital and Clinics, Department of Neurosurgery, Iowa city, IOWA, USA
[c] Neuroimaging and Interventional Radiology, National Institute for Mental Health and Neurosciences (NIMHANS), Bengaluru, India

ARTICLE INFORMATION

Article history:
Received 28 November 2019
Accepted 7 May 2020

Spinal cord lesions are traditionally classified as either extradural or intradural extramedullary or of intramedullary origin. Intramedullary spinal cord tumours are histopathologically similar to cranial tumours with a diverse range of pathologies. Astrocytomas and ependymomas account for approximately 80% of all intramedullary tumours, with other primary and secondary lesions accounting for the remaining 20%. Magnetic resonance imaging is the preferred imaging modality for diagnosing and characterising spinal cord lesions; however, accurate characterisation of tumour histology can be challenging, and is further confounded by intramedullary non-neoplastic lesions, such as demyelinating vascular, inflammatory, infectious, or traumatic lesions. This review illustrates the spectrum of intramedullary tumours and tumour mimics with emphasis on the imaging findings.

Introduction

Intramedullary tumours account for 20–30% of all primary intradural tumours and 2–4% of all primary central nervous system (CNS) tumours.[1,2] Gliomas (astrocytoma and ependymoma) account for 80% of all intramedullary tumours, haemangioblastomas 3–8%, metastasis 2% followed by other rare lesions including primary CNS lymphomas, and melanomas[2,3]; however, accurate characterisation of tumour histology can be challenging, and is further confounded by non-tumour lesions (demyelination, infection, etc.), which may nevertheless mimic an intramedullary mass.[4,5] As cord biopsy is an invasive high-risk procedure, imaging plays an important role in the preoperative assessment of tumours.[5] The following sections review the pertinent imaging findings in common and uncommon intramedullary tumours and tumour mimics with illustrative examples. (Table 1)

Spinal cord tumours

Typical imaging findings of a spinal cord tumour on magnetic resonance imaging (MRI) is a solid lesion with variable enhancement causing enlargement of the cord accompanied by cysts and surrounding syrinx/oedema. The cysts can be either tumoural or non-tumoural (polar) in origin. Tumoural cysts are located within the tumoural mass and result from necrosis, liquefaction, and degeneration.[6] They have variable signal intensity and may not always follow the low T1-weighted imaging (WI) and high T2WI signal intensity. There is accompanying peripheral enhancement, useful to differentiate from non-tumoural

* Guarantor and correspondent: S.G. Kandemirli, University of Iowa Hospital and Clinics, Department of Radiology, Iowa, USA. Tel.: +1 319 9300850.
E-mail address: sedat-kandemirli@uiowa.edu (S.G. Kandemirli).

https://doi.org/10.1016/j.crad.2020.05.010
0009-9260/

Table 1
Imaging features of intramedullary tumours and tumour mimics.

	Location, Demographics	Imaging features
Ependymoma	- Cervical, thoracic	Central location, well-defined margin T1 shortening due to haemorrhage Hypointense rim due to haemorrhage on T2WI (cap sign; 20–45%) - polar (21.7–90%) and tumoural (22–52.2%) cysts are common
Astrocytoma	Thoracic levels in adults Cervical/cervicothoracic cord in paediatric - Holocord	More eccentric location compared to ependymomas Infiltrative margins Cysts are less common compared to ependymoma Focal/patchy enhancement - cap sign less common (10%)
Ganglioglioma	Cervical, thoracic Cervicomedullary extension - Holocord	Eccentric in location Heterogeneous signal on T1WI Tumoural cysts (46%) more common compared to astrocytomas and ependymomas Patchy enhancement, may reach to pial surface - calcification
Haemangioblastoma	Thoracic, cervical Usually solitary - Multiple in VHL	Dorsal intramedullary location Vascular flow-voids (if >15 mm) - extensive cord oedema and syringohydromyelia out of proportion to lesion size
Metastasis	Thoracic, cervical Solitary - Primary lung (50%), breast (30%)	Extensive cord oedema Rim and flame signs - rare cyst formation
Lymphoma	Leptomeningeal disease invading cord Primary intramedullary spinal cord lymphoma is exceptionally rare - mainly seen in conus medullaris/cauda equine	Poorly circumscribed hyperintense signal on T2WI No accompanying cystic or haemorrhagic component - concurrent cranial enhancing lesions suggestive of CNS lymphoma are supportive findings
Lipoma	Associated with dysraphism Intradural epicentre with intramedullary extension - Dorsal location at cervicothoracic level	Hyperintense on T1WI and hypointense on T2WI, follows signal characteristics of fat - no enhancement
Multiple sclerosis	- Asian-type MS higher rate of syrinx compared to western-type MS	Dorsolateral cord, less than half of the cross-sectional area of cord - less than two vertebral segments in length
Transverse myelitis	- thoracic	Central, more than two-thirds of the cross-sectional area of cord - more than two vertebral segments (commonly 3–4) in length
Cord abscess	- Associated with immunosuppression, dysraphism, adjacent infection	Hypointense on T1WI, hyperintense on T2WI with surrounding cord oedema and expansion Low T2 signal of abscess capsule - internal restricted diffusion
Neurosarcoidosis	Cervical, thoracic	Imaging findings depend on stage of involvement Long segment with predilection for dorsal surface Leptomeningeal enhancement Fusiform expansion of cord with hyperintense signal on T2WI - patchy or diffuse intramedullary enhancement
Cavernoma	- Thoracic	Eccentric location Heterogeneous signal intensity centrally on T1WI and T2WI, “popcorn” lesion - absence of enhancement
Dural AVF	- Thoracolumbar	Feeder: radiculomeningeal artery Cord oedema starting from conus medullaris Vascular flow voids (on T2WI) or enhancing vessels (on contrast-enhanced T1WI) - cord swelling with atrophic changes in long-term

cysts. Tumoural cysts require resection during surgery with the solid tumoural mass, as they can be lined with abnormal glial cells.[7] Polar cysts, on the other hand, are located at cranial or caudal poles of the solid portion of the tumour, do not enhance, and result from blockage of cerebrospinal fluid (CSF) flow. Polar cysts are non-septate and do not have echogenic walls at intraoperative ultrasonography. They do not need to be excised surgically and may decompress upon removal of the solid tumour or they can be aspirated during resection.[6]

Ependymoma

Ependymoma is the most common intramedullary tumour in adults and accounts for 60–70% of all intramedullary glial tumours.[2] It is uncommon in paediatric population, except for patients with neurofibromatosis type 2.[8,9] Ependymomas originate from ependymal cells lining the central canal. The distinguishing feature is displacement, rather than infiltration of adjacent neural tissue. This creates a cleavage plane and facilitates surgical resection.[10] There are three categories based on World Health Organization (WHO) classification: grade 1 includes myxopapillary ependymoma and subependymoma; grade 2 is the classic ependymoma; and grade 3 is anaplastic ependymoma. Except for the myxopapillary variant, there is a predilection for cervical and thoracic cord.[11–13]

On MRI, lesions are iso-to hypointense on T1WI (occasionally, T1 shortening due to haemorrhage may occur) and hyperintense on T2WI (Fig 1). The lesions are centrally located with majority (77%) having well-defined margins.[13] The mean lesion length is 3.4–3.7 vertebrae.[13,14] Majority shows some degree of contrast enhancement, which may be homogeneous (75%), heterogeneous, rim, or nodular pattern.[15] In 20–45% of cases, a hypointense rim due to haemorrhage is seen on T2WI (cap sign).[10,14,15] Both polar (21.7–90%) and tumoural cysts (22–52.2%) are a common feature.[10,13,16] Syringohydromyelia is also common (10–50%).[15] Central location, homogeneous enhancement, and haemorrhage at margins are useful clues to differentiate from astrocytomas.

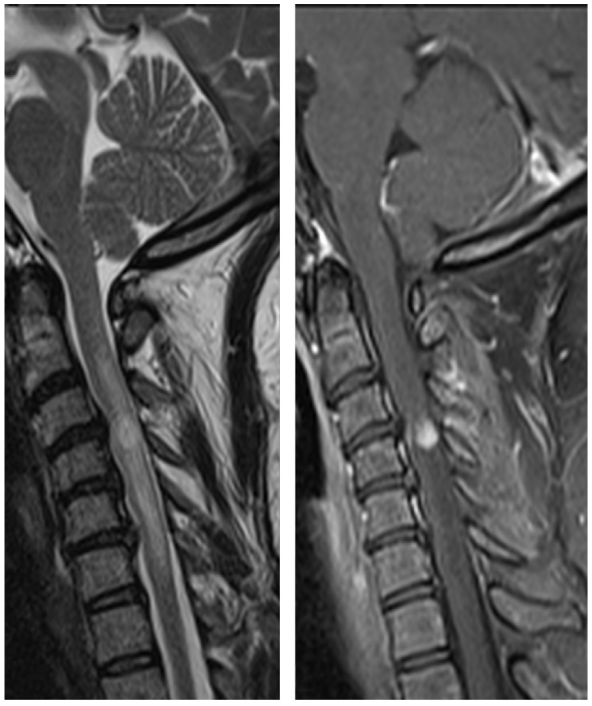

Figure 2 Pilocytic astrocytoma (WHO grade I). (a) Sagittal T2WI and (b) contrast-enhanced T1WI shows a T2 hyperintense lesion enhancing homogeneously at C3–C4 level with surrounding oedema.

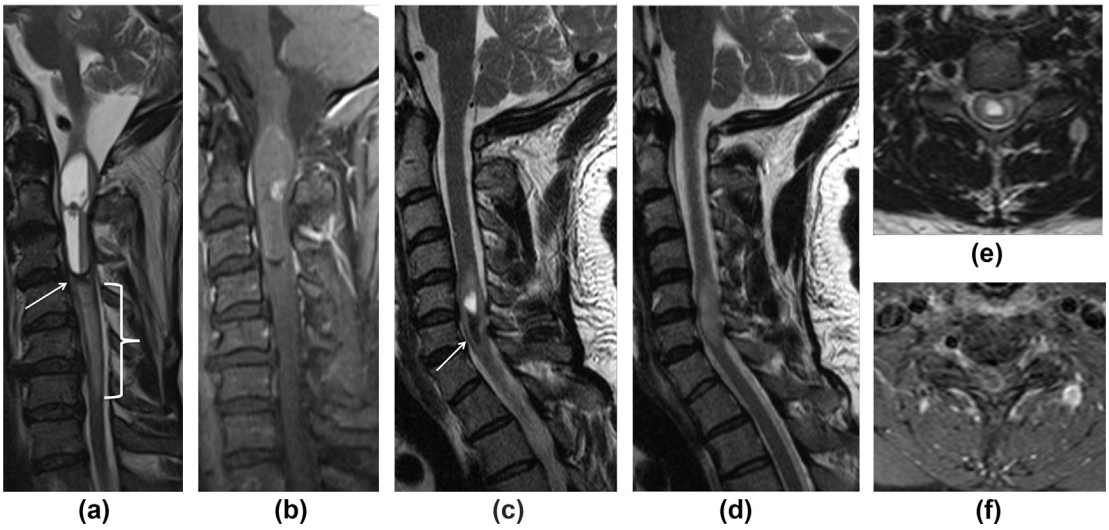

Figure 1 Ependymoma (WHO grade II). (a) Sagittal T2WI shows a well-defined predominantly cystic lesion at C2–C3 level with fluid–fluid level and haemosiderin rim (arrow). There is accompanying cord oedema (bracket). (b) Contrast-enhanced sagittal T1WI shows focal enhancing tumour nodule. (c–f) Another patient with grade II ependymoma (Tanycytic variant). (c) Midline and (d) paramidline sagittal T2WI shows a lesion at C5–C6 level both with solid and cystic components and a haemosiderin cap (arrow). Axial T2WI (e) and contrast-enhanced T1WI (f) show fluid–fluid level and rim enhancement. Unlike the prior case, no surrounding cord oedema is seen.

Figure 3 Diffuse astrocytoma (WHO grade II). (a) Sagittal T2WI shows an expansile cord lesion at T5–T8 levels with multiple internal cysts. Rostrally, there is atrophic cord with increased signal (bracket). (b) On contrast-enhanced T1WI, there was no enhancement. Surgical resection was difficult due to the infiltrative nature of the tumour.

Astrocytoma

Astrocytomas account for 30–40% of intramedullary glial tumours in adults and approximately 82% of intramedullary tumours in children.[2] They are classified into four WHO grades: pilocytic (grade I), fibrillary (grade II), anaplastic (grade III) and glioblastoma (grade IV).[10] Grade I and II astrocytomas (Figs 2 and 3) account for majority (75%) of cases and grade III (anaplastic) lesions (Fig 4) account for approximately 25%.[17] Spinal glioblastomas (Fig 5) are rare (0.2–1.5%).[17] Unlike ependymomas, astrocytomas are more infiltrative and creating a surgical cleavage plane is more difficult.[17] There is a predilection for thoracic levels in adults, and cervical/cervicothoracic cord in paediatric population.[18] Holocord involvement may be seen in children.[8]

Astrocytomas have a more eccentric location compared to ependymomas. On MRI, lesions have poorly defined margins and are iso-to-hypointense on T1WI and hyperintense on T2WI.[18,19] The average length of lesions is four vertebrae.[20] Cysts of either polar or tumoural varieties are less common compared to ependymomas.[14] The majority of lesions enhance, although enhancement is often focal or patchy.[8,14] The cap sign may be seen occasionally (10%).[14] Diffusion-weighted imaging (DWI) can be used to differentiate between low and high-grade tumours with high-grade tumours showing lower ADC values.[21]

Ganglioglioma

Gangliogliomas are composed of glial cells and dysplastic neurons.[22] Spinal gangliogliomas account for 1.1% of all intramedullary tumours.[23] They are seen more frequently in children and are the second most common intramedullary tumour after astrocytoma in the paediatric population.[8] Lesions often involve the cervical and thoracic cord.[8,23] There is a predilection for cervicomedullary extension (Fig 6) and holocord involvement (Fig 7).[8]

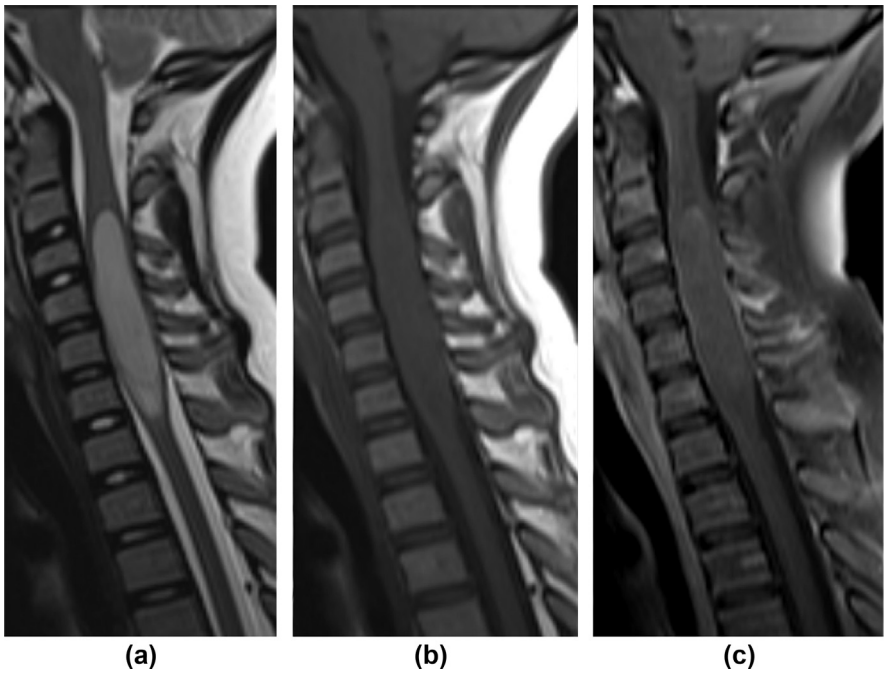

Figure 4 Anaplastic astrocytoma (WHO grade III). (a) Sagittal T2WI and (b) pre-contrast T1WI show a fusiform, homogeneous expansile cord lesion at C3–C6 levels with no accompanying cord oedema. (c) Post-contrast T1WI reveals mild, diffuse patchy enhancement. On surgical resection, cleavage plane was preserved except at the caudal aspect of the lesion.

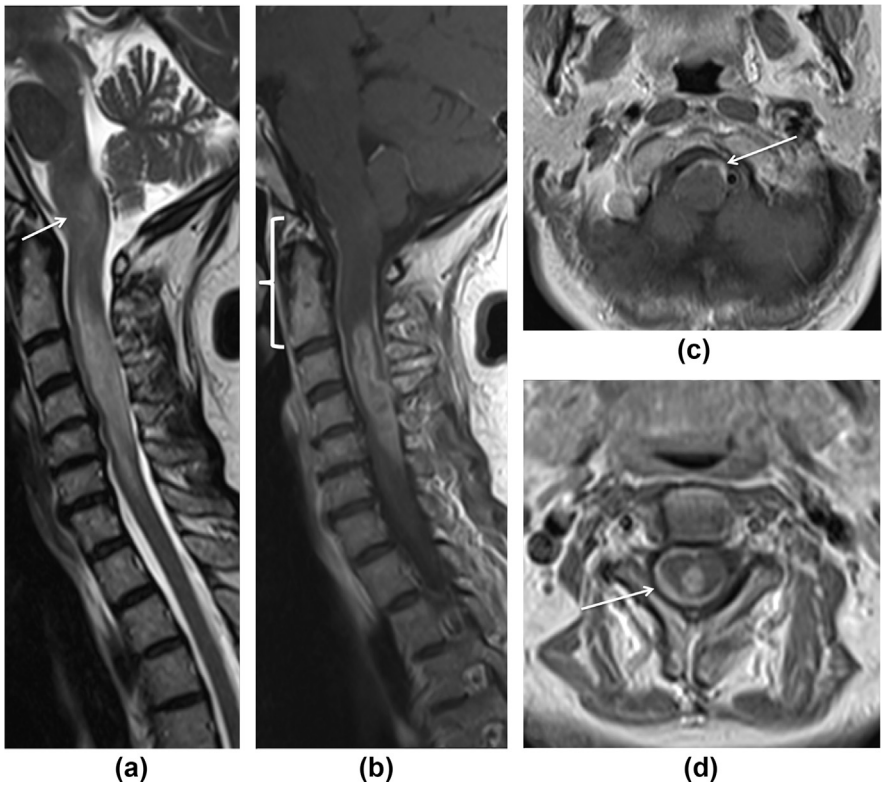

Figure 5 Glioblastoma multiforme in a 67-year-old woman presenting with paraesthesia. (a) Sagittal T2WI shows fusiform lesion expanding the cord with indistinct margins at C2–C6 levels, with signal changes extending to cervicomedullary junction (arrow). (b–d) Contrast-enhanced T1WI shows heterogeneous enhancement of the intramedullary lesion, along with leptomeningeal spread (bracket in b and arrows in c and d). During surgical resection, grossly thickened arachnoid was noted.

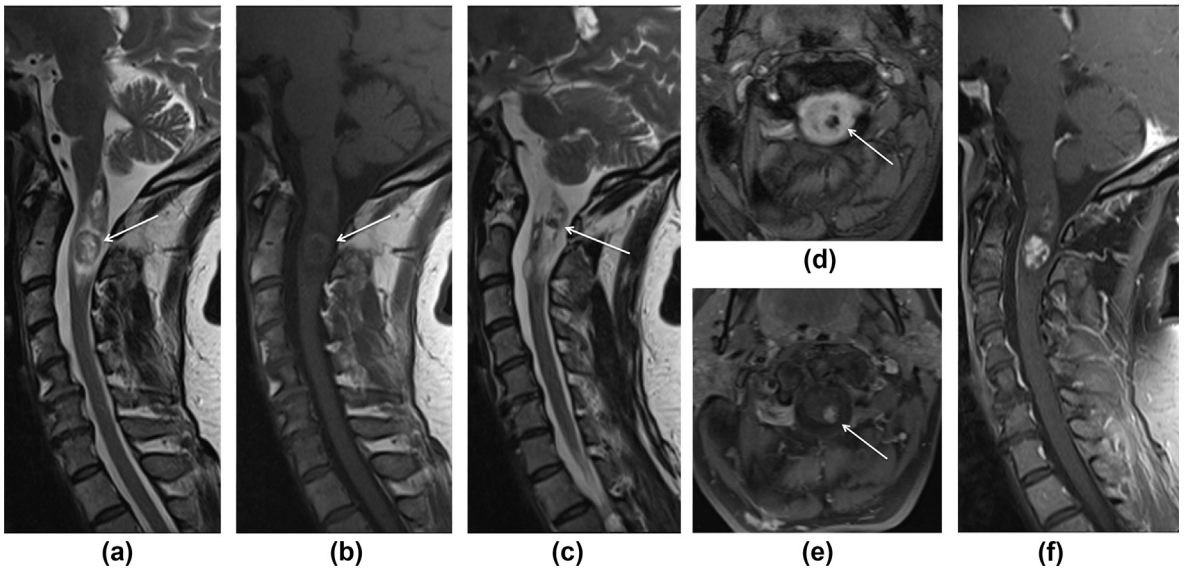

Figure 6 Ganglioglioma (WHO grade I) in a 48-year-old woman with upper extremity paraesthesia. (a) Sagittal T2WI and (b) T1WI show a lesion at the C2 level with a hypointense T2 (arrow) and hyperintense on T1WI rim (arrow). There is extension into the cervicomedullary junction. (c) Left paramidline sagittal T2WI and (d) axial GRE sequences show eccentrically located haemorrhagic component (arrow) and enhancement reaching up to pial surface (e, arrow). (f) Sagittal contrast-enhanced T1WI shows heterogeneous enhancement.

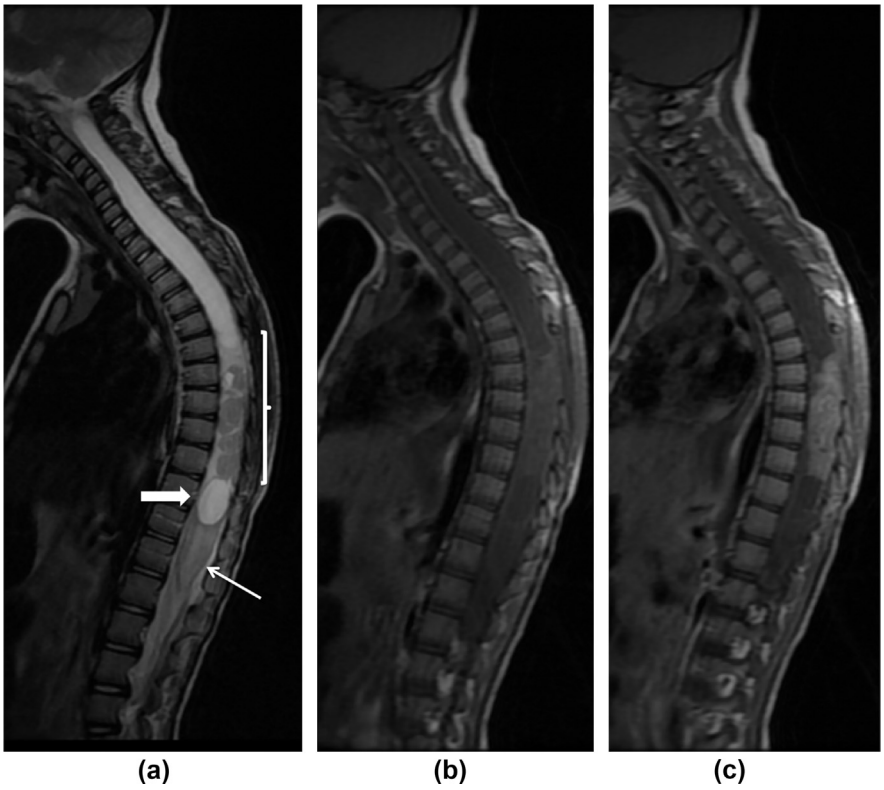

Figure 7 Ganglioglioma (WHO grade I) in a 4-year-old patient with progressive lower extremity weakness. (a) Sagittal T2WI shows a heterogeneous lesion at T6–T10 level (bracket). There is syrinx formation rostrally extending to the cervicomedullary junction. There is a caudal cyst (block arrow), which do not show enhancement, consistent with non-tumoural cyst. There is cord oedema caudally extending to conus medullaris (arrow). (b) Unenhanced and (c) contrast-enhanced T1WI shows diffuse enhancement of the solid component.

Gangliogliomas are commonly eccentric in location.[23] Heterogeneous signal intensity on T1WI (possibly reflecting different cell lineage types) may be a useful imaging clue.[23] There is less surrounding oedema compared to astrocytomas and ependymomas. Tumoural cysts, however, occur with greater frequency (46%) compared to astrocytomas and ependymomas.[23] Enhancement often is patchy and may reach up to pial surface.[23] Calcification, although less frequent compared to cranial gangliogliomas, may be seen.[23]

Haemangioblastoma

Spinal haemangioblastomas (WHO grade I) account for 1.6–5.8% of all spinal tumours.[24,25] They are often solitary.[25] Multiple haemangioblastomas may occur in association with von Hippel–Lindau syndrome.[26] A differentiating presenting feature, though rare, is subarachnoid or intramedullary haemorrhage.[27,28]

Lesions are mainly located thoracic and cervical levels.[26] Haemangioblastomas may have different morphologies including: (1) intramedullary location with syringomyelia (seen in 40%) and cord enlargement, (2) haemangioblastoma originating from the cord surface with exophytic growth and little reaction in the adjacent cord (snowman sign on contrast-enhanced images), (3) haemangioblastoma exclusively in the extramedullary space.[26,29] Dorsal intramedullary location near the surface of spinal cord predominates.[29]

Lesions are typically iso-to hypointense on T1WI, and iso-to-hyperintense on T2WI. Vascular flow-voids may be seen, especially in tumours >15 mm.[24,26] Smaller lesions show homogeneous enhancement, whereas large lesions enhance heterogeneously.[9,24] Extensive cord oedema and syringohydromyelia out of proportion to lesion size, possibly related to arteriovenous shunting or venous congestion, are helpful imaging clues (Fig 8).[26]

Metastasis

Intramedullary metastases from non-CNS primaries are rare with a reported frequency of 0.9–2.1% on autopsy series.[30,31] The majority are from a lung primary (50%), followed by breast.[32,33] These may occur secondary to haematogenous dissemination, retrograde venous spread, perineural lymphatic spread, or direct invasion.[32] Majority of spinal cord metastases is solitary and often localised to thoracic or cervical cord (80%).[32]

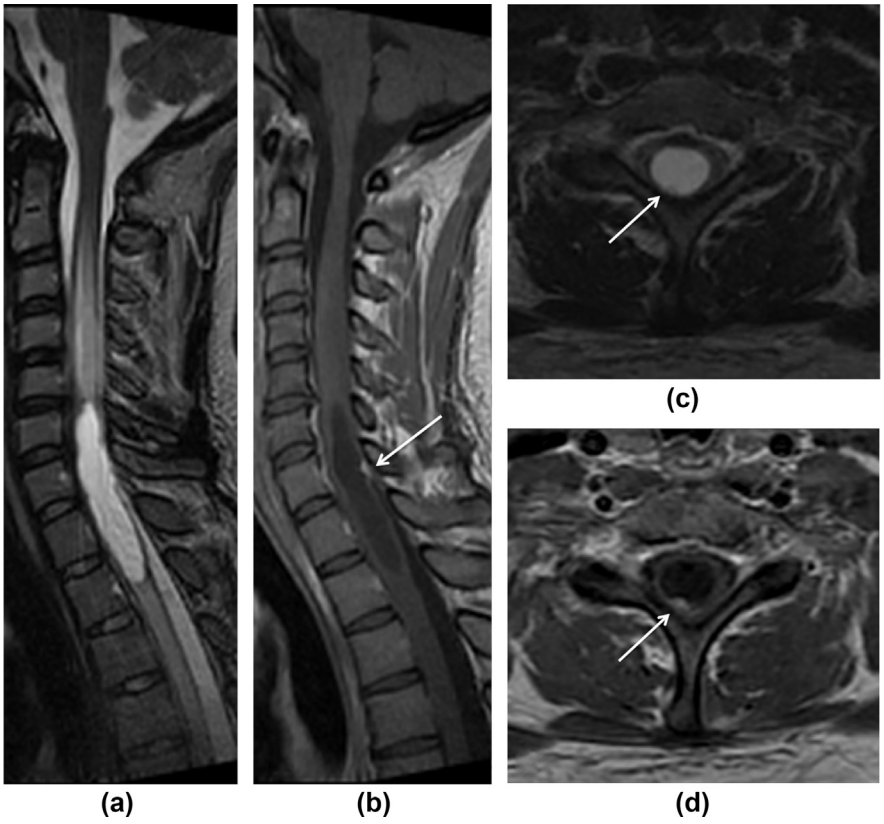

Figure 8 Haemangioblastoma in a 28-year-old with back pain. (a) Sagittal and (c) axial T2WI show syrinx formation at C6–T2 level with extensive surrounding cord oedema. (c) There is a hypointense focus on dorsal pial surface noted on T2WI (arrow). (b,d) On the contrast-enhanced images, this nodule shows homogeneous enhancement. Surgical resection confirmed haemangioblastoma. Note the extensive syrinx formation and cord oedema out of proportion to lesion size.

Lesions are isointense on T1WI and hyperintense on T2WI. Unlike primary intramedullary tumours, cyst formation is rare (3%).[32] These lesions often have extensive surrounding cord oedema (mean 4.5 segments) and prominent contrast enhancement.[32] Additionally described imaging findings include rim and flame signs (Fig 9).[34] The rim sign denotes thin peripheral enhancement more intense than central enhancement, and occurs more commonly in metastasis (33%) compared to other cord tumours (3%).[34] Flame sign describes ill-defined tapering enhancement at the poles of the lesion and is again more common in metastasis (30%) than other cord tumours (3%).[34]

Lymphoma

Intramedullary lymphoma may present as leptomeningeal disease invading the spinal cord or primary CNS lymphoma.[35] Primary intramedullary spinal cord lymphoma is an exceptionally rare disease and comprises only 1–3% of all CNS lymphomas.[36,37] They are mainly of B-cell origin lymphoma, with the most common type being diffuse large B-cell lymphoma (40–50% of cases).[38] Primary intramedullary spinal cord lymphoma has predilection for conus medullaris/cauda equina involvement.[39]

On MRI, intramedullary lesions are poorly circumscribed with isointense signal on T1WI, and hyperintense signal on T2WI (Fig 10).[35,39] Enhancement is variable and may be patchy, confluent, or discrete.[35] There is usually no accompanying cystic or haemorrhagic component, distinguishing from other glial tumours.[35] Concurrent enhancing lesions suggestive of CNS lymphoma on cranial MRI are supportive findings.[39]

Uncommon intramedullary masses

Lipoma

Spinal lipomas typically are extradural and seen in association with spinal dysraphism. Intramedullary cord lipomas without dysraphism are rare, and usually have an intradural epicentre with intramedullary extension. Total surgical resection is difficult, as there is typically no clear plane of cleavage between lipoma, cord, and nerve roots. Lipomas are located dorsally with a predilection for cervicothoracic level.[40]

Lipomas are hyperintense on T1WI and hypointense on T2WI and tend to follow signal characteristics of fat with no enhancement (Fig 11).[41] Short T1 inversion recovery (STIR), or T1-fat suppressed sequences can be used to illustrate the fatty nature of the mass.

Figure 9 Spinal cord metastasis in a 54-year-old woman with progressive lower extremity weakness and history of uterine carcinoma. (a) Sagittal T2WI shows a relatively homogeneous lesion centred at C4–C5 levels. There is extensive surrounding cord oedema. (b) Contrast-enhanced image shows heterogeneous internal enhancement along with rim sign (curved arrow) and flame sign (arrows).

Figure 10 Primary CNS lymphoma in a 46-year-old man with primary cerebral CNS lymphoma, presenting with progressive paraesthesia. (a) Sagittal T2WI shows patchy areas of increased signal intensity without significant cord expansion. (b) On the contrast-enhanced image, there is marked confluent homogeneous enhancement.

Melanotic lesions

Melanotic schwannoma, meningeal melanocytoma, blue nevus of the CNS, and primary melanoma constitute the primary pigmented tumours of the CNS, and can be difficult to differentiate from each other.[42,43] Primary melanoma in CNS is unusual (1% of all melanoma cases), with intramedullary location ever rarer.[43]

Melanomas generally are iso-to slightly hyperintense on T1WI, and hypointense on T2WI (Fig 12). They mainly involve the thoracic cord and show homogeneous enhancement.[42,44] Intra-lesional haemorrhage may be seen. Overall, the MRI signal depends on degree of melanin content and presence of haemorrhage.[43]

Autograft-derived intramedullary mass

Human neural stem cells derived from olfactory mucosa may be used on experimental basis in patients with spinal cord injuries.[45] Olfactory mucosa contains stem-like progenitor cells and olfactory ensheathing cells thought to mediate repair of the CNS. Olfactory mucosal stem cells have been shown to be effective in regenerating neuronal cell populations *in vitro*; however, the long-term effects are unknown, and based on rare case reports, there is concern for de-novo tumour formation from these transplanted stem cells.[45,46]

Imaging findings are rather non-specific showing hyperintense expansive mass with cystic components and subtle, patchy contrast-enhanced enhancement (Fig 13). A prior history of stem cell transplant could be the only clue to the aetiology of the mass.

Tumour mimics

Although spinal cord tumours have some distinguishing features, in some cases it can be challenging to differentiate spinal cord tumours from intramedullary non-neoplastic lesions, which may have underlying demyelinating vascular, inflammatory, infectious (Electronic Supplementary Material Fig. S1) or traumatic aetiologies.

Demyelinating disease

Demyelinating lesions may be seen in multiple sclerosis (MS), neuromyelitis optica spectrum disorders, acute transverse myelitis, and acute disseminated encephalomyelitis. MS accounts for more than half of demyelinating lesions in the spinal cord and isolated spinal cord involvement can occur in 10–20% of cases. Lesions cover less than half of cross-sectional area with a dorsolateral predilection and extend less than two vertebral segments in length.[4] There can be accompanying rim or patchy enhancement in active lesions. Occasionally, demyelinating lesions may mimic an expansile mass with accompanying syrinx (Fig 14).[47,48] Asian-type MS may have a higher rate of syrinx formation compared to western-type MS.[47] Such cases of

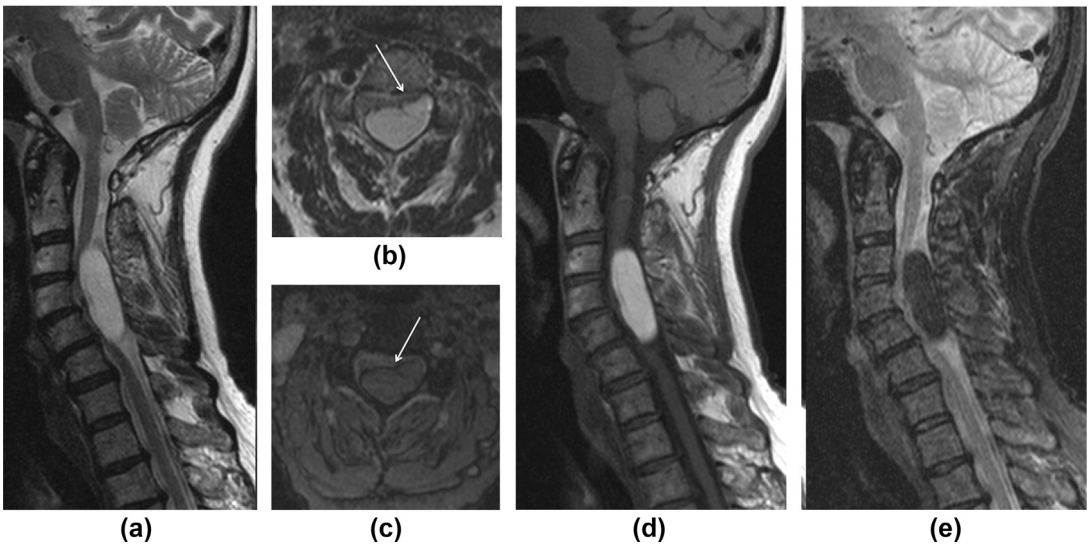

Figure 11 Spinal cord lipoma. (a) Sagittal T2WI shows an intradural T2 hyperintense lesion displacing the cord anteriorly. (b) Axial T2WI shows intramedullary extension. (c) GRE exaggerates the chemical shift artefact between the lesion and spinal cord. (d) Sagittal T1WI and (e) STIR images again confirming intralesional fat. During surgical exploration, rostral parts of the lipoma could not be totally resected due to the absence of a cleavage plane.

expansile demyelinating lesions can be difficult to distinguish from spinal cord gliomas on MRI and CSF analysis; and erroneously or intentionally undergo biopsy.[47,48] Advanced imaging techniques, such as diffusion tensor imaging (DTI) or perfusion weighted imaging (PWI), may be helpful to differentiate between demyelinating lesion and spinal masses.[49,50] The latter have lower fractional anisotropy values.[50] In addition, demyelinating lesions do not disrupt the white matter tracts (streamlines) on DTI.[49] On perfusion imaging, spinal cord tumours have higher peak height values compared to demyelinating lesions.[50]

Acute transverse myelitis (ATM) has a central location and covers more than two-thirds of the cross-sectional area of the spinal cord with a craniocaudal extent of more than two vertebral segments (commonly three to four).[4] The thoracic cord is the most commonly affected site.

Acute disseminated encephalomyelitis (ADEM) is an acute, monophasic condition with a predilection for the paediatric population. In up to one-third of patients, there

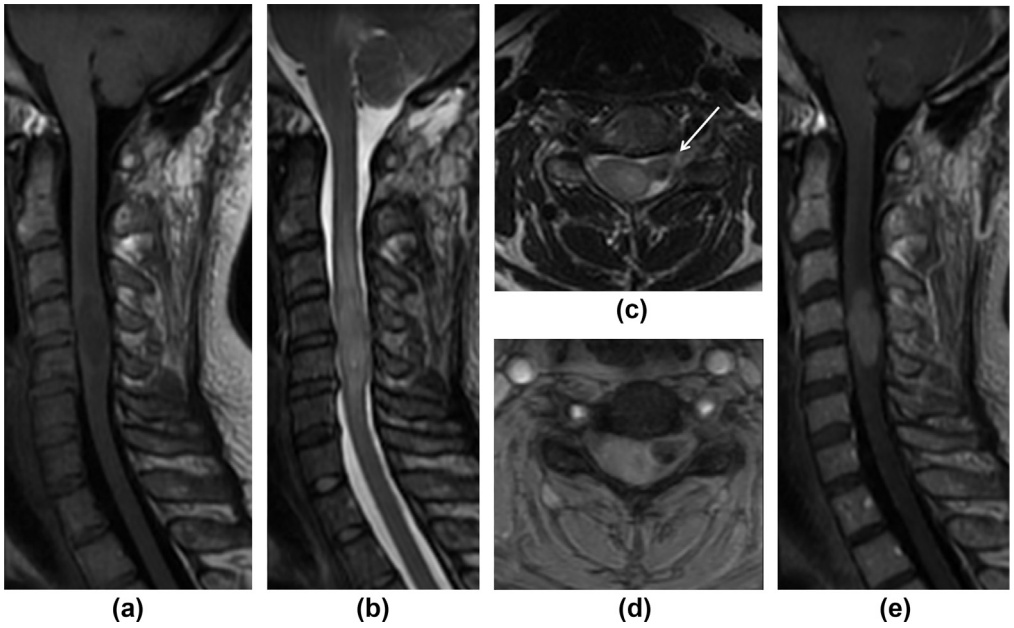

Figure 12 Primary CNS melanoma. (a) Sagittal T1WI shows an expansile lesion with subtle rim hyperintensity at C4–C5 level. (b) Sagittal T2WI shows expansile cord lesion with surrounding short segment cord oedema. (c) Axial T2WI and (d) GRE imaging show the intra-axial component and a haemorrhagic exophytic component. (e) The lesion shows homogeneous contrast enhancement.

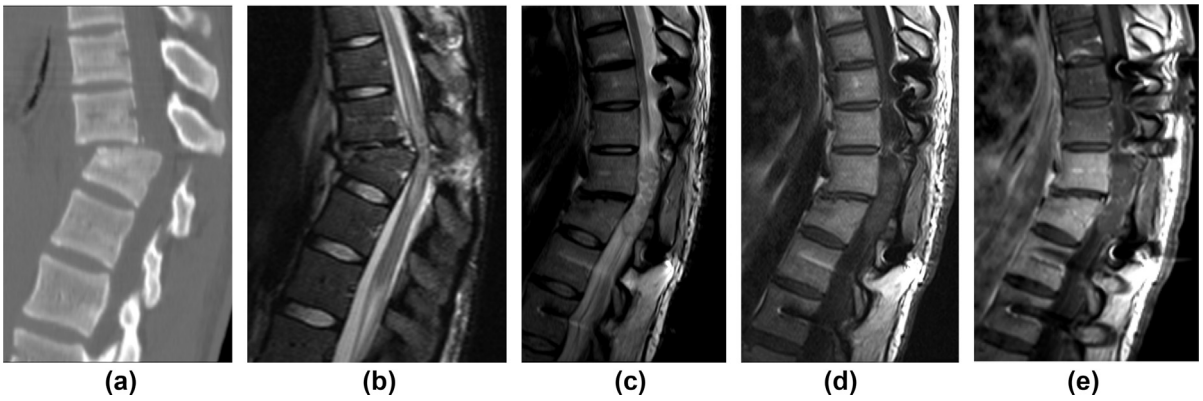

Figure 13 An 18-year-old woman with T10–11 fracture dislocation secondary to motor vehicle accident. (a) There is retropulsion of the vertebral body with extensive cord oedema (b) at presentation. Three years later, the patient underwent stem cell implant derived from olfactory mucosa into spinal cord. A few years later, the patient presented with worsening back pain. (c) Sagittal T2WI, (d) unenhanced, and (e) contrast-enhanced images show hyperintense expansile mass with cystic components and subtle, patchy contrast-enhanced enhancement (e). Pathology demonstrated respiratory epithelium and submucosal glands with goblet cells, suggesting origin of the mass from implanted cells.

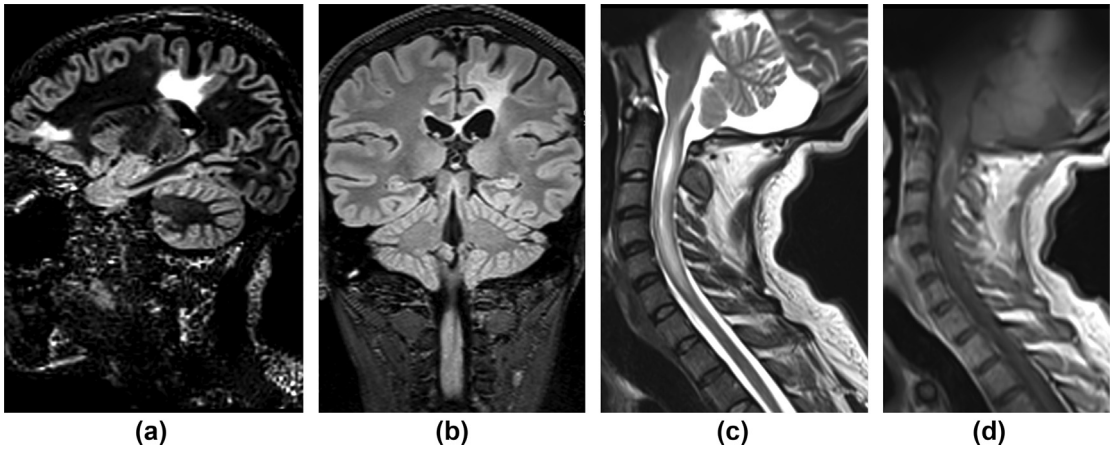

Figure 14 Demyelinating lesion mimicking tumour. (a) Sagittal double inversion recovery and (b) coronal FLAIR images show multiple demyelinating lesions in frontal and parietal lobes. (c) On sagittal T2WI there is a hyperintense lesion centred at C2–C3 levels with accompanying cord expansion. (d) Contrast-enhanced image shows rim enhancement. Both intracranial and spinal lesions responded to medical therapy.

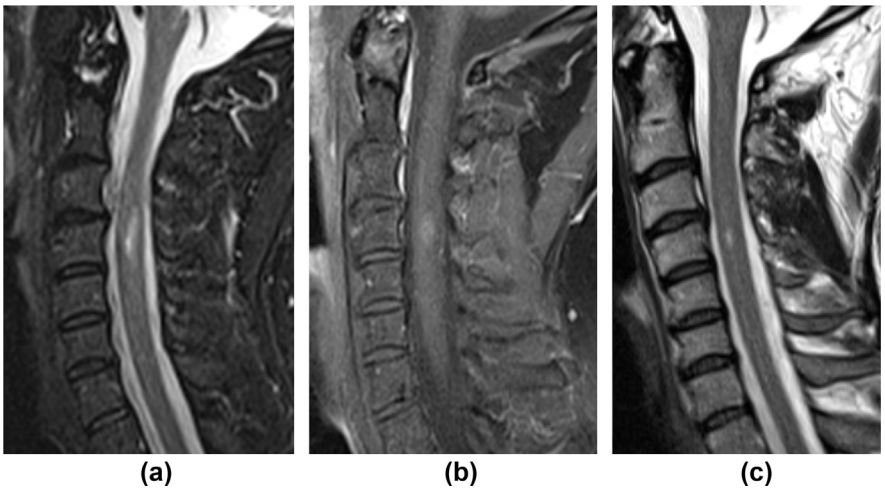

Figure 15 Cord injury secondary to cervical nerve block. (a) Initial sagittal STIR and (b) contrast-enhanced images show a short segment lesion at C4 level with faint enhancement. Follow-up imaging 6-months later shows regression of signal abnormality.

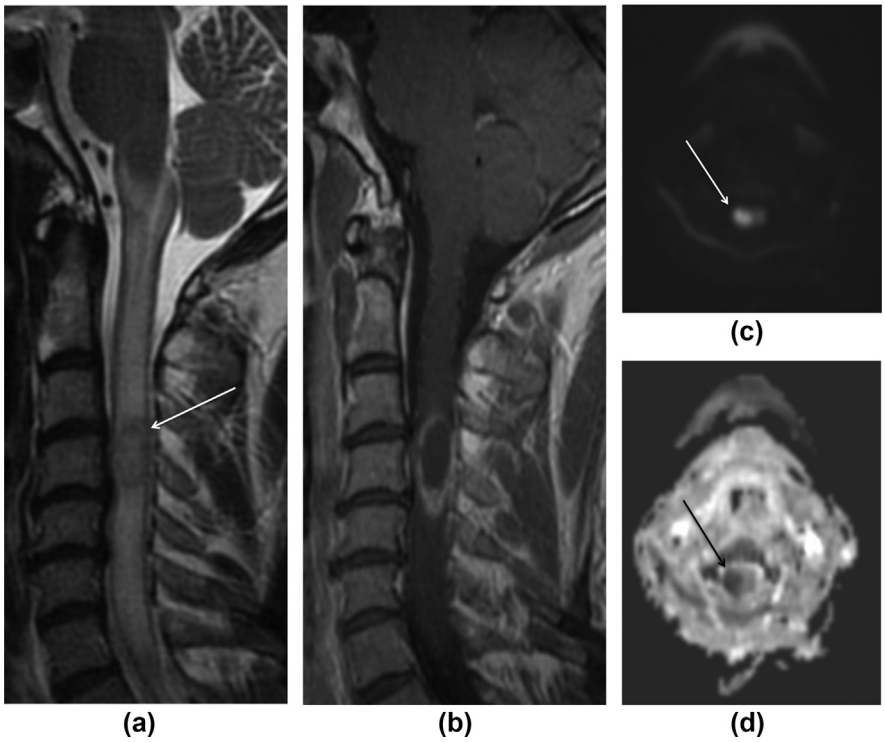

Figure 16 Spinal cord abscess. Sagittal T2WI shows a lesion with hypointense rim (arrow). There is associated cord expansion and marked oedema. (b) Contrast-enhanced images show rim enhancement of the lesion. (c) DWI and (d) ADC map show diffusion restriction (arrows) of the central necrotic component. Surgical specimen and CSF sampling grew *Aggregatibacter aphrophilus/paraphrophilus* possibly from an oral or gastrointestinal source.

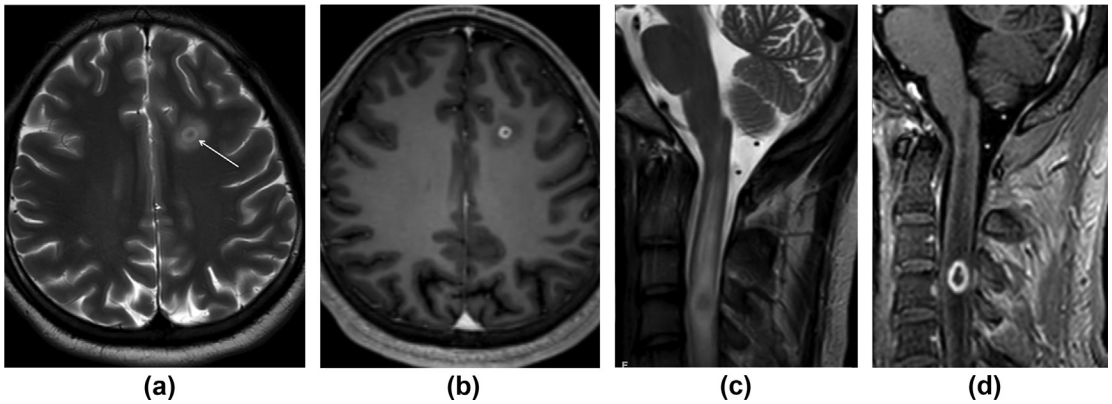

Figure 17 Tuberculoma. (a) Axial T2WI shows a frontal nodular lesion characterised by outer T2 hypointense rim (arrow), inner hyperintense rim, and hypointense centre. (b) There is rim enhancement contrast-enhanced. (c) Sagittal T2WI at cervical level shows a T2 hypointense lesion, again with rim enhancement (d).

can be myelitis in addition to intracranial findings. Spinal cord lesions are confluent in appearance with cord swelling or lesions can have a pattern similar to transverse myelitis.[5]

Cord injury

Main mechanism of injury to spinal cord is myelopathic spondylosis and spinal canal stenosis. Occasionally, the injury may be iatrogenic. This can result in focal signal abnormality in the affected cord. There is typically focal T2 hyperintensity at level of spinal stenosis, with or without associated enhancement. Cases with cord oedema, haematoma and/or enhancement may mimic tumours.[4] Other mechanisms of cord injuries may present with similar imaging findings (Fig 15).

Infection

Cord abscess

Intramedullary spinal cord abscess is rare. Under normal circumstances, the spinal cord is resistant to

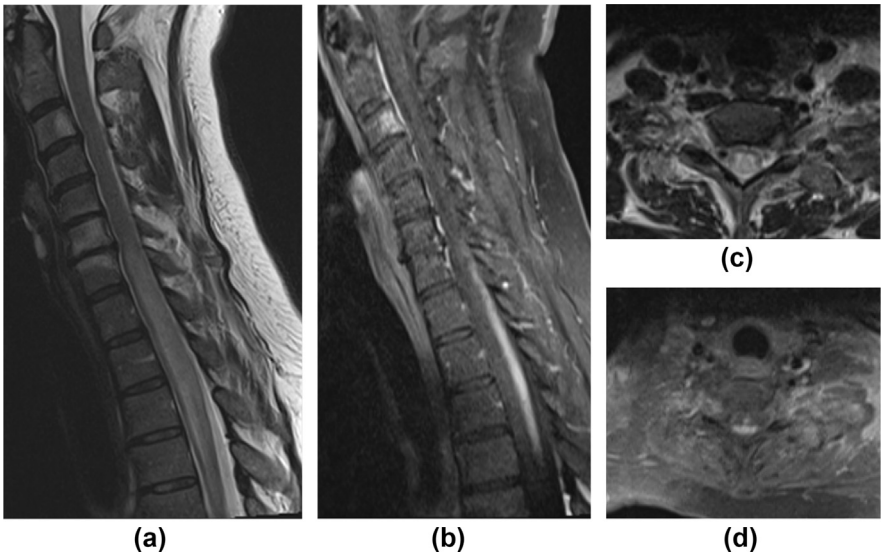

Figure 18 Neurosarcoidosis in a 50-year-old woman with back pain and lower extremity weakness. (a) Sagittal and (c) axial T2WI show long segment, diffuse cord signal abnormality with associated cord expansion. (b,d) On contrast-enhanced images there is diffuse enhancement mainly at dorsal pial surface and also centrally. The patient was treated with steroids with good response.

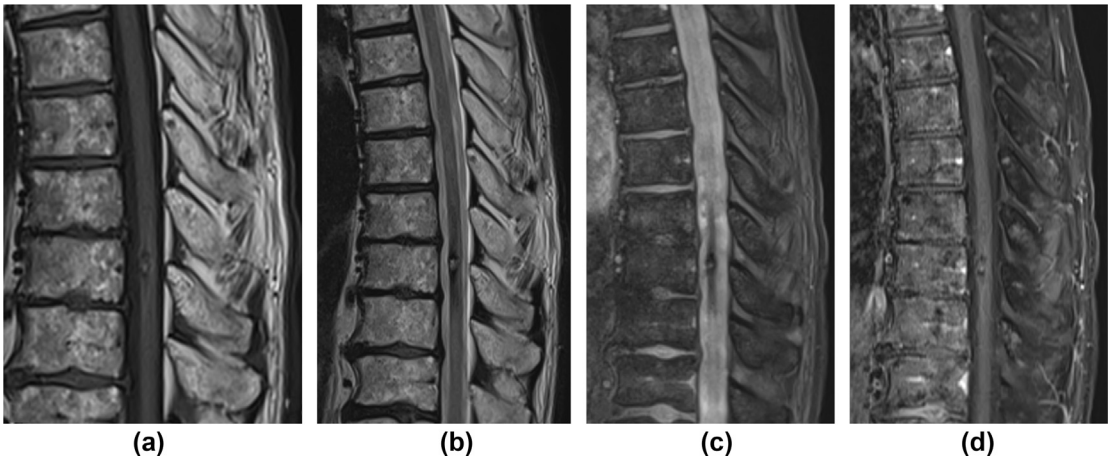

Figure 19 Cavernoma. (a) Sagittal T1WI and (b) T2WI show an intramedullary lesion with spontaneous hyperintensity on T1WI and hypointense periphery on T2WI suggestive of haemosiderin products. (c) Sagittal GRE confirms blood products by showing marked blooming artefact. (d) On contrast-enhanced images, no enhancement is seen.

infection. Abscess usually results only from immunosuppression, structural abnormality (such as dysraphism), or adjacent infection.[51] Spinal cord abscesses are hypointense on T1WI and hyperintense on T2WI with surrounding cord oedema and expansion. Low T2 signal along the abscess capsule and presence of restricted diffusion on DWI are helpful imaging clues. Rim-enhancement is typically present (Fig 16).[52]

Tuberculosis

Spinal intramedullary tuberculoma accounts for 0.2% of all CNS tuberculosis.[53] The majority of cases involve the thoracic cord.[54] MRI findings depend on the presence of caseation and liquefaction. Non-caseating tuberculoma are T1 isointense, T2 hyperintense and enhance homogeneously. Caseating, non-liquefied granulomas are iso-to hypointense on both T1-and T2WI, while caseating, liquefied granulomas are hypointense on T1WI and hyperintense on T2WI centrally. Caseating granulomas show rim enhancement (Fig 17).[55]

Spinal neurosarcoidosis

CNS involvement occurs in 5–15% of symptomatic sarcoidosis patients.[56] Spinal cord involvement usually occurs with brain involvement, isolated spinal involvement being rare.[56] In Junger's classification for spinal cord involvement, different stages of spinal cord involvement

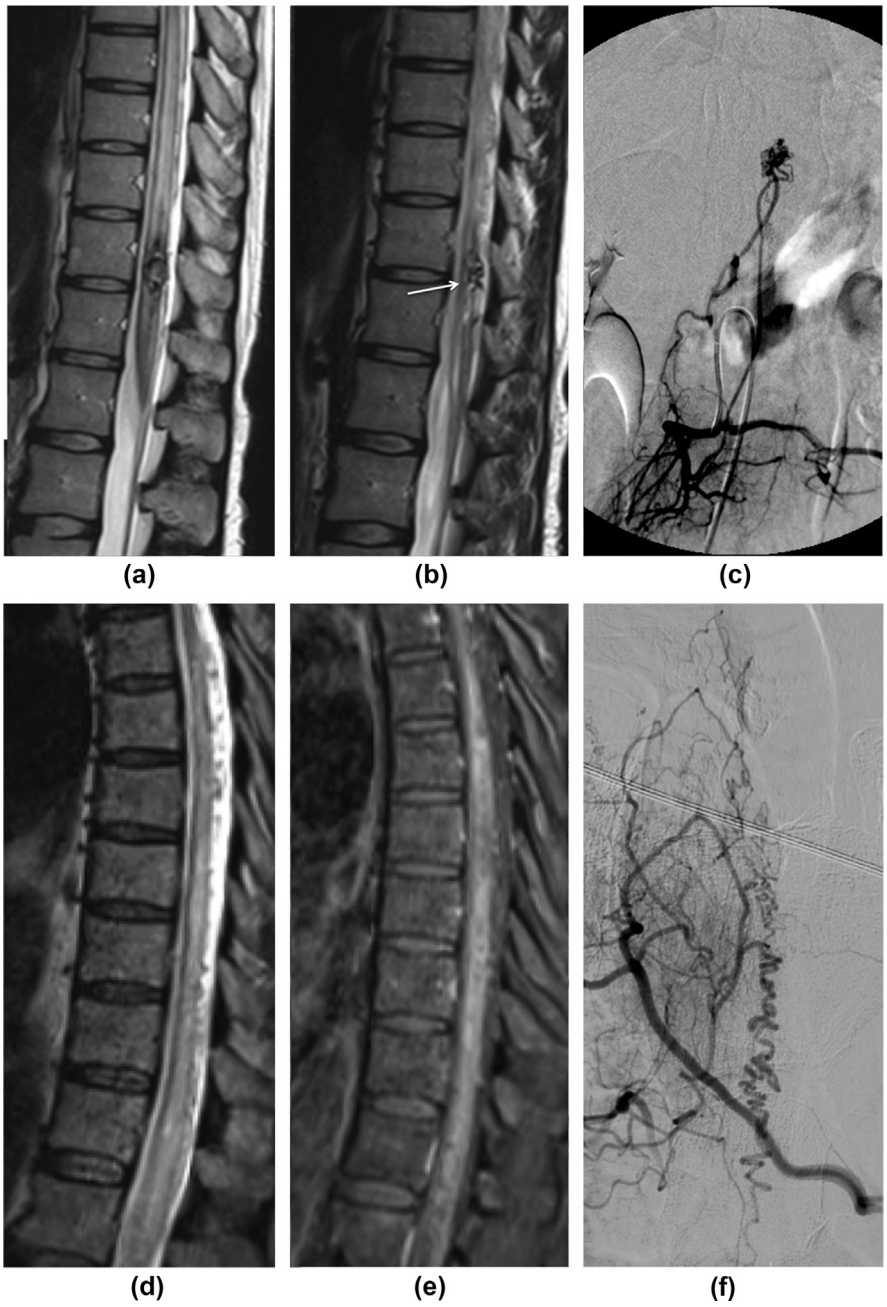

Figure 20 (a–c) Intramedullary AVM. (a) Sagittal T2WI show a heterogeneous intramedullary lesion with surrounding haemosiderin. (b) More lateral sagittal T2WI shows tortuous vessels (arrow) suggestive of underlying AVM. (c) Selective angiogram through the right L2 pedicle shows intramedullary AVM. The patient was treated with Onyx embolisation. (d–f) Dural arteriovenous fistula. (d) Sagittal T2WI and (e) contrast-enhanced T1WI show diffusely increased spinal cord intensity on T2WI extending throughout the cord. On contrast-enhanced images, there is accompanying diffuse enhancement. Note is also made of perimedullary flow voids on T2WI that are also seen as enhancing vessels on contrast-enhanced images. (f) Selective angiogram through the right L4 pedicle shows dural arteriovenous fistula with network of dilated perimedullary veins. (Courtesy of Osman Kizilkilic, Istanbul University, Cerrahpasa Faculty of Medicine.)

have been described, progressing through stages of leptomenigeal enhancement; parenchymal involvement with cord enhancement and cord swelling; resolution of cord swelling with residual focal areas of intramedullary enhancement; and resolution of inflammation with normal size or atrophy of the spinal cord with no enhancement.[57]

Spinal cord sarcoidosis has a predilection for cervical and thoracic levels.[56] MRI findings depend on stage of involvement and include leptomeningeal enhancement, fusiform expansion of cord with hyperintense signal on T2WI with patchy or diffuse intramedullary enhancement (Fig 18).[58] Involvement is often long segment with predilection for dorsal surface.[56]

Vascular

Cavernoma

Cavernomas (cavernous angioma) are characterised by thin-walled dilated sinusoidal spaces without intervening neural tissue.[59] They account for 3–5% of intramedullary lesions in adults.[60] There is a predilection for thoracic cord.[61] Blood products in various stages of evolution cause heterogeneous signal intensity centrally on T1-and T2WI, resulting in "popcorn" lesions (Fig 19). Intramedullary lesions usually have an eccentric location.[59] Enhancement is typically absent, although minimal enhancement may be seen. The lesions often have peripheral low signal intensity due to haemosiderin deposition. Gradient echo sequences can demonstrate the haemorrhagic content. Surrounding cord oedema is uncommon without recent haemorrhage. Ependymomas may mimic cavernomas due to haemorrhage associated with ependymomas. Useful differentiating features of cavernomas include small size (usually less than one vertebra), eccentric location, minimal enhancement, and absence of oedema.[59]

Vascular malformation

Spinal vascular malformations can be classified based on type of feeding artery. Dural arteriovenous fistulae (dAVF) are fed by radiculomeningeal arteries, whereas pial arteriovenous malformations (AVM) are supplied by radiculomedullary and radiculopial arteries.[62] Spinal dAVFs are the most commonly encountered spinal vascular malformation, accounting for 70% of cases.[62] There is usually an acquired shunt between a radiculomeningeal artery and a radicular vein. Thoracolumbar region is the most common site for fistulae. Main pathology involves retrograde drainage into perimedullary vessels with decreased arteriovenous pressure gradient with decreased drainage of normal spinal veins. This ultimately results in venous congestion with intramedullary oedema. MRI shows cord oedema starting from conus level and perimedullary dilated vessels. Oedema is seen as centromedullary, ill-defined hyperintensity on T2WI over multiple segments. There might be contrast enhancement related to chronic venous congestion and ischaemia (Fig 20). The cord may have a swollen appearance with atrophic changes in chronic cases. Perimedullary vessels are usually seen as flow voids on T2WI and enhancing tortuous vessels on contrast-enhanced images; however, in small shunt volume or fistula located at cervical level, flow voids may not be detected on T2WI and seen only in contrast-enhanced series.[63] In selective digital subtraction angiography, after catheterisation of the fistula level, early venous filling and retrograde contrast medium opacification of the radiculomedullary veins are visualised. There is also opacification of dilated perimedullary veins.

Spinal cord AVM are congenital in origin and less frequent compared to dural AVFs.[62,64] Depending on the type of transition between artery and vein, pial AVMs can be divided into glomerular and fistulous types. Glomerular type AVMs have an intramedullary nidus (Fig 20). Fistulous AVMs (perimedullary fistula type) are characterised by direct shunts superficially around the spinal cord, rarely with associated intramedullary component.[62,64] Spinal cord AVMs usually involve the thoracolumbar region and show mixed heterogeneous signal on T1-and T2WI due to blood products. The surrounding T2 hyperintensity, often a combination of oedema, gliosis, and infarction, can cause cord enlargement and mimic a tumour-like lesion. The nidus shows variable degree of enhancement. A differentiating feature is the presence of serpentine flow voids and enhancement both within and at cord surface due to tortuous feeding vessels and draining veins.[62,64]

Radiation myelopathy

Patients with primary or metastatic intramedullary or extramedullary spinal tumours may receive radiation therapy. Clinical deterioration in such patients may occur on follow-up. Diagnostic studies can be inconclusive on the underlying aetiology, whether there is tumour recurrence or radiation myelopathy. The distinction between recurrence and radiation effect is challenging, requiring a multidisciplinary approach. Knowledge of the radiation dose and ports is necessary in establishing the diagnosis of radiation myelopathy.[65]

Conclusion

Intramedullary spinal cord abnormalities include a variety of tumour and tumour-like conditions. Understanding the main differentiating features between tumours and tumour-like conditions is essential to avoid unnecessary intervention. In case of spinal cord tumour, presence of cleavage plane, differentiation between neoplastic and polar cysts; and distinction between cord oedema and tumour are important points for assessment.

Conflict of Interest

The authors declare no conflict of interest.

Appendix A. Supplementary data

Supplementary data to this article can be found online at https://doi.org/10.1016/j.crad.2020.05.010.

References

1. Duong LM, McCarthy BJ, McLendon RE, *et al*. Descriptive epidemiology of malignant and nonmalignant primary spinal cord, spinal meninges, and cauda equina tumours, United States, 2004-2007. *Cancer* 2012;**118**:4220–7.
2. Grimm S, Chamberlain MC. Adult primary spinal cord tumours. *Expert Rev Neurother* 2009;**9**:1487–95.
3. Tobin MK, Geraghty JR, Engelhard HH, *et al*. Intramedullary spinal cord tumours: a review of current and future treatment strategies. *Neurosurg Focus* 2015;**39**:E14.
4. Maj E, Wojtowicz K, Aleksandra, *et al*. Intramedullary spinal tumour-like lesions. *Acta Radiol* 2019;**60**:994–1010.
5. Mohajeri Moghaddam S, Bhatt AA. Location, length, and enhancement: systematic approach to differentiating intramedullary spinal cord lesions. *Insights Imaging* 2018;**9**:511–26.
6. Kahan H, Sklar EM, Post MJ, *et al*. MR characteristics of histopathologic subtypes of spinal ependymoma. *AJNR Am J Neuroradiol* 1996;**17**:143–50.
7. Goy AM, Pinto RS, Raghavendra BN, *et al*. Intramedullary spinal cord tumours: MR imaging, with emphasis on associated cysts. *Radiology* 1986;**161**:381–6.
8. Rossi A, Gandolfo C, Morana G, *et al*. Tumours of the spine in children. *Neuroimaging Clin N Am* 2007;**17**:17–35.
9. Merhemic Z, Stosic-Opincal T, Thurnher MM. Neuroimaging of spinal tumours. *Magn Reson Imaging Clin N Am* 2016;**24**:563–79.
10. Koeller KK, Rosenblum RS, Morrison AL. Neoplasms of the spinal cord and filum terminale: radiologic–pathologic correlation. *RadioGraphics* 2000;**20**:1721–49.
11. Klekamp J. Spinal ependymomas. Part 1: intramedullary ependymomas. *Neurosurg Focus* 2015;**39**:E6.
12. Raco A, Esposito V, Lenzi J, *et al*. Long-term follow-up of intramedullary spinal cord tumours: a series of 202 cases. *Neurosurgery* 2005;**56**:972–81.
13. Sun B, Wang C, Wang J, *et al*. MRI features of intramedullary spinal cord ependymomas. *J Neuroimaging* 2003;**13**:346–51.
14. Kim DH, Kim JH, Choi SH, *et al*. Differentiation between intramedullary spinal ependymoma and astrocytoma: comparative MRI analysis. *Clin Radiol* 2014;**69**:29–35.
15. Kobayashi K, Ando K, Kato F, *et al*. Variety of preoperative MRI changes in spinal cord ependymoma of WHO grade II: a case series. *Eur Spine J* 2019;**28**:426–33.
16. Dauleac C, Messerer R, Obadia-Andre N, *et al*. Cysts associated with intramedullary ependymomas of the spinal cord: clinical, MRI and oncological features. *J Neurooncol* 2019;**144**:385–91.
17. Huisman TA. Pediatric tumours of the spine. *Cancer Imaging* 2009;**9**:S45–8.
18. Ledbetter LN, Leever JD. Imaging of intraspinal tumours. *Radiol Clin North Am* 2019;**57**:341–57.
19. Horger M, Ritz R, Beschorner R, *et al*. Spinal pilocytic astrocytoma: MR imaging findings at first presentation and following surgery. *Eur J Radiol* 2011;**79**:389–99.
20. Babu R, Karikari IO, Owens TR, *et al*. Spinal cord astrocytomas: a modern 20-year experience at a single institution. *Spine (Phila Pa 1976)* 2014;**39**:533–40.
21. Hasan DI, Abowarda MH, Taha MM. Diffusion-weighted MRI and apparent diffusion coefficient value in assessment of intra-medullary spinal cord masses. *Egypt J Radiol Nucl Med* 2016;**47**:1575–84.
22. Gessi M, Dorner E, Dreschmann V, *et al*. Intramedullary gangliogliomas: histopathologic and molecular features of 25 cases. *Hum Pathol* 2016;**49**:107–13.
23. Patel U, Pinto RS, Miller DC, *et al*. MR of spinal cord ganglioglioma. *AJNR Am J Neuroradiol* 1998;**19**:879–87.
24. Chu BC, Terae S, Hida K, *et al*. MR findings in spinal haemangioblastoma: correlation with symptoms and with angiographic and surgical findings. *AJNR Am J Neuroradiol* 2001;**22**:206–17.
25. Peckham ME, Hutchins TA. Imaging of vascular disorders of the spine. *Radiol Clin North Am* 2019;**57**:307–18.
26. Baker KB, Moran CJ, Wippold 2nd FJ, *et al*. MR imaging of spinal haemangioblastoma. *AJR Am J Roentgenol* 2000;**174**:377–82.
27. Berlis A, Schumacher M, Spreer J, *et al*. Subarachnoid haemorrhage due to cervical spinal cord haemangioblastomas in a patient with von Hippel–Lindau disease. *Acta Neurochir (Wien)* 2003;**145**:1009–13.
28. Koda M, Mannoji C, Itabashi T, *et al*. Intramedullary haemorrhage caused by spinal cord haemangioblastoma: a case report. *BMC Res Notes* 2014;**7**:823.
29. Imagama S, Ito Z, Wakao N, *et al*. Differentiation of localization of spinal haemangioblastomas based on imaging and pathological findings. *Eur Spine J* 2011;**20**:1377–84.
30. Chason JL, Walker FB, Landers JW. Metastatic carcinoma in the central nervous system and dorsal root ganglia. A prospective autopsy study. *Cancer* 1963;**16**:781–7.
31. Costigan DA, Winkelman MD. Intramedullary spinal cord metastasis. A clinicopathological study of 13 cases. *J Neurosurg* 1985;**62**:227–33.
32. Rykken JB, Diehn FE, Hunt CH, *et al*. Intramedullary spinal cord metastases: MRI and relevant clinical features from a 13-year institutional case series. *AJNR Am J Neuroradiol* 2013;**34**:2043–9.
33. Sung WS, Sung MJ, Chan JH, *et al*. Intramedullary spinal cord metastases: a 20-year institutional experience with a comprehensive literature review. *World Neurosurg* 2013;**79**:576–84.
34. Rykken JB, Diehn FE, Hunt CH, *et al*. Rim and flame signs: postgadolinium MRI findings specific for non-CNS intramedullary spinal cord metastases. *AJNR Am J Neuroradiol* 2013:34908–15.
35. Haque S, Law M, Abrey LE, *et al*. Imaging of lymphoma of the central nervous system, spine, and orbit. *Radiol Clin North Am* 2008;**46**:339–61.
36. Koeller KK, Smirniotopoulos JG, Jones RV. Primary central nervous system lymphoma: radiologic–pathologic correlation. *RadioGraphics* 1997;**17**:1497–526.
37. Feng L, Chen D, Zhou H, *et al*. Spinal primary central nervous system lymphoma: case report and literature review. *J Clin Neurosci* 2018;**50**:16–9.
38. Yang W, Garzon-Muvdi T, Braileanu M, *et al*. Primary intramedullary spinal cord lymphoma: a population-based study. *Neuro Oncol* 2017;**19**:414–21.
39. Flanagan EP, O'Neill BP, Porter AB, *et al*. Primary intramedullary spinal cord lymphoma. *Neurology* 2011;**77**:784–91.
40. Bhatoe HS, Singh P, Chaturvedi A, *et al*. Nondysraphic intramedullary spinal cord lipomas: a review. *Neurosurg Focus* 2005;**18**:Ecp1.
41. Cavusoglu M, Ciliz DS, Duran S, *et al*. Intramedullary lipoma of the cervico-thoracic spinal cord. *JBR-BTR.* 2014;**97**:346–8.
42. Karikari IO, Powers CJ, Bagley CA, *et al*. Primary intramedullary melanocytoma of the spinal cord: case report. *Neurosurgery* 2009;**64**:E777–8.
43. Farrokh D, Fransen P, Faverly D. MR findings of a primary intramedullary malignant melanoma: case report and literature review. *AJNR Am J Neuroradiol* 2001;**22**:1864–6.
44. Painter TJ, Chaljub G, Sethi R, *et al*. Intracranial and intraspinal meningeal melanocytosis. *AJNR Am J Neuroradiol* 2000;**21**:1349–53.
45. Dlouhy BJ, Awe O, Rao RC, *et al*. Autograft-derived spinal cord mass following olfactory mucosal cell transplantation in a spinal cord injury patient: case report. *J Neurosurg Spine* 2014;**21**:618–22.
46. Amariglio N, Hirshberg A, Scheithauer BW, *et al*. Donor-derived brain tumour following neural stem cell transplantation in an ataxia telangiectasia patient. *PLoS Med* 2009;**6**:e1000029.
47. Waziri A, Vonsattel JP, Kaiser MG, *et al*. Expansile, enhancing cervical cord lesion with an associated syrinx secondary to demyelination. Case report and review of the literature. *J Neurosurg Spine* 2007;**6**:52–6.
48. Lee M, Epstein FJ, Rezai AR, *et al*. Nonneoplastic intramedullary spinal cord lesions mimicking tumours. *Neurosurgery* 1998;**43**:788–94.
49. Egger K, Hohenhaus M, Van Velthoven V, *et al*. Spinal diffusion tensor tractography for differentiation of intramedullary tumour-suspected lesions. *Eur J Radiol* 2016;**85**:2275–80.

50. Liu X, Tian W, Kolar B, *et al*. Advanced MR diffusion tensor imaging and perfusion weighted imaging of intramedullary tumours and tumour like lesions in the cervicomedullary junction region and the cervical spinal cord. *J Neurooncol* 2014;**116**:559–66.
51. Hood B, Wolfe SQ, Trivedi RA, *et al*. Intramedullary abscess of the cervical spinal cord in an otherwise healthy man. *World Neurosurg* 2011;**76**. 361.e315-369.
52. Bakhsheshian J, Kim PE, Attenello FJ. Intramedullary cervical spinal cord abscess. *World Neurosurg* 2017;**106**:e1041–9.
53. Liu J, Zhang H, He B, *et al*. Intramedullary tuberculoma combined with abscess: case report and literature review. *World Neurosurg* 2016;**89**. 726.e721-724.
54. Nussbaum ES, Rockswold GL, Bergman TA, *et al*. Spinal tuberculosis: a diagnostic and management challenge. *J Neurosurg* 1995;**83**:243–7.
55. Lu M. Imaging diagnosis of spinal intramedullary tuberculoma: case reports and literature review. *J Spinal Cord Med* 2010;**33**:159–62.
56. Soni N, Bathla G, Pillenahalli Maheshwarappa R. Imaging findings in spinal sarcoidosis: a report of 18 cases and review of the current literature. *Neuroradiology J* 2019;**32**:17–28.
57. Junger SS, Stern BJ, Levine SR, *et al*. Intramedullary spinal sarcoidosis: clinical and magnetic resonance imaging characteristics. *Neurology* 1993;**43**:333–7.
58. Do-Dai DD, Brooks MK, Goldkamp A, *et al*. Magnetic resonance imaging of intramedullary spinal cord lesions: a pictorial review. *Curr Probl Diagn Radiol* 2010;**39**:160–85.
59. Jeon I, Jung WS, Suh SH, *et al*. MR imaging features that distinguish spinal cavernous angioma from haemorrhagic ependymoma and serial MRI changes in cavernous angioma. *J Neurooncol* 2016;**130**:229–36.
60. El-Koussy M, Stepper F, Spreng A, *et al*. Incidence, clinical presentation and imaging findings of cavernous malformations of the CNS. A twenty-year experience. *Swiss Med Wkly* 2011;**141**:w13172.
61. Ren J, Hong T, He C, *et al*. Surgical approaches and long-term outcomes of intramedullary spinal cord cavernous malformations: a single-center consecutive series of 219 patients. *J Neurosurg Spine* 2019:1–10.
62. Krings T. Vascular malformations of the spine and spinal cord: anatomy, classification, treatment. *Clin Neuroradiol* 2010;**20**:5–24.
63. Miller TR, Eskey CJ, Mamourian AC. Absence of abnormal vessels in the subarachnoid space on conventional magnetic resonance imaging in patients with spinal dural arteriovenous fistulas. *Neurosurg Focus* 2012;**32**:E15.
64. Krings T, Lasjaunias PL, Hans FJ, *et al*. Imaging in spinal vascular disease. *Neuroimaging Clin N Am* 2007;**17**:57–72.
65. Gibbs IC, Patil C, Gerszten PC, *et al*. Delayed radiation-induced myelopathy after spinal radiosurgery. *Neurosurgery* 2009;**64**:67–72.